Environmental Science Processes & Impacts

ROYAL SOCIETY OF CHEMISTRY

PAPER

View Article Online
View Journal

Cite this: DOI: 10.1039/d5em00912j

Dynamic variability of CO_2 emissions from agricultural canal-lake systems in cold and arid regions

Ying Wang,[ab] Wenzhu Yang [ab] and Yan Jiao *[ab]

Agricultural canal-lake systems are potential hotspots for greenhouse gas (GHG) emissions; however, existing studies have largely focused on natural water bodies or single-type water bodies, with limited research on the continuum. Therefore, this study analyzed the dynamics of CO_2 flux (F_{CO_2}) in the agricultural canal-Lake Ulansuhai continuum within the Hetao Irrigation District of Inner Mongolia and quantified the annual CO_2 emissions ($F_{CO_2 total}$) from agricultural canals and lakes on the Inner Mongolia Plateau. The results showed that agricultural canals were persistently supersaturated with CO_2 and released it to the atmosphere, with their average F_{CO_2} (49.43 ± 37.28 mmol per m^2 per day) being significantly higher than that of the connected Lake Ulansuhai and the average level of Chinese lakes. Although the average F_{CO_2} of Lake Ulansuhai was higher than that of major freshwater lakes in China, some areas of the lake acted as a net CO_2 sink during the autumn irrigation period, revealing a dynamic shift between a carbon source and sink in cold-arid lakes. The annual CO_2 emissions from agricultural canals and lakes on the Inner Mongolia Plateau were 0.0097 Tg C per year and 0.22 Tg C per year, respectively, providing key baseline data for regional carbon budgeting. This study transcends the limitations of traditional fragmented research approaches by systematically quantifying the differences in CO_2 emissions between canals and lakes within the continuum and highlights the role of agricultural canal-lake systems as regional carbon emission hotspots. The findings provide a scientific basis for salinization control, eutrophication prevention, and water environment protection of the Yellow River, and also offer critical data support for regional ecological management and carbon accounting in cold and arid regions.

Received 5th November 2025
Accepted 28th April 2026

DOI: 10.1039/d5em00912j

rsc.li/espi

Environmental significance

Agricultural canal-lake systems are potential hotspots for greenhouse gas (GHG) emissions, yet existing studies have largely focused on single-type water bodies, with limited research on the continuum. This study systematically elucidated the CO_2 emission dynamics of agricultural canal-lake systems in cold and arid regions. The findings provided a data foundation for carbon accounting of inland waters in typical agricultural areas of China and offered scientific management support for the restoration of the "mountains–waters–forests–farmlands–lakes–grasslands–deserts" system on the Inner Mongolia Plateau, as well as for addressing salinization and eutrophication in Lake Ulansuhai.

1. Introduction

Carbon is widely distributed across various spheres of the Earth, including the atmosphere, rocks, organisms, and water bodies, and plays a central role in biogeochemical cycles. Global inland waters, encompassing rivers, lakes, reservoirs, estuaries, and coastal wetlands, cover 2.67% of the Earth's surface and represent a crucial source of greenhouse gas (GHG) emissions.[1–5] Furthermore, GHG emissions from inland waters increase with agricultural activities, reaching peak levels particularly in agriculturally intensive regions.[6–8]

China accounts for 8.64% of the global arable land area.[9] With the expansion of agricultural production and the increase in fertilization and irrigation activities, the number and area of agricultural canals have also expanded. These canals serve as transitional zones between irrigation, drainage, farmland runoff, and rivers and lakes. Their prominent characteristics include frequent wet-dry alternation, high sediment content, and the transport of large amounts of soluble nutrients such as carbon and nitrogen. As such, they are sites of highly active biogeochemical processes.[6,10–12] Furthermore, they exhibit morphological features similar to small still water bodies. Compared to natural systems (streams, lakes, and ponds),

[a]College of Chemistry and Environmental Science, Inner Mongolia Normal University, No. 81 Zhaowuda Road, Hohhot 010022, China. E-mail: jiaoyan@imnu.edu.cn
[b]Inner Mongolia Key Laboratory of Environmental Chemistry, Inner Mongolia Normal University, No. 81 Zhaowuda Road, Hohhot 010022, China

canals have higher emissions per unit area.[13] Specifically, the global warming potential (GWP) of agricultural canals (10.9 g CO_2-eq per m^2 per days) is more than double that of global ponds (4.7 g CO_2-eq per m^2 per days) and comparable to that of agricultural reservoirs (11.1 g CO_2-eq per m^2 per days).[6] Previous research had indicated that global methane emissions from ditches account for approximately 1% of all anthropogenic methane emissions.[14] However, the relative contributions of ditch systems to CO_2 emissions at regional and global scales remain unknown.[15] In addition, the factors related to carbon emissions from ditches were also unclear.[11] The Hetao Irrigation District in Inner Mongolia is a large irrigation district located upstream of the Yellow River. Within the entire irrigation and drainage engineering system, there are over 80 000 water intake canals used for irrigation. Part of this irrigation water leaks into the ground, while the rest flows through nearly 20 000 drainage canals and eventually enters Ulansuhai Lake *via* major drainage canals. This region serves as a typical area for studying carbon emissions from agricultural canals in the cold and arid regions of China.[16]

Lakes, as critical components of freshwater ecosystems, account for only 3.7% of the global non-glaciated land area, yet they accumulate substantial carbon pools. By regulating the cycling balance between surface water, groundwater, and precipitation, they serve as critical nexuses in regional carbon cycles. Furthermore, these water bodies function not only as vital sites for carbon storage, migration, and transformation but also as key emission sources of CO_2 and CH_4.[17] Globally, lakes release 0.11–0.57 Pg C per year into the atmosphere, constituting a significant source of atmospheric CO_2.[19,20] The lakes in Inner Mongolia are mainly divided into five watersheds based on water resource zoning: the Songhua River Basin, the Liao River Basin, the Hai River Basin, the Yellow River Basin, and the northwestern river basins. According to the Water Resources Census of Inner Mongolia Autonomous Region, the List of Lakes in Inner Mongolia Autonomous Region, and the Handbook of River and Lake Characteristics in Inner Mongolia Autonomous Region, there are a total of 655 lakes in the region. The lakes within the river basins of Inner Mongolia Autonomous Region mainly include 163 lakes, such as Ulansuhai Lake, Hongjiannao Lake, and Hasuhai Lake. In the 2010s, the total area of lakes larger than 10 km^2 on the Inner Mongolia Plateau was 4213.24 km^2.

The Inner Mongolia Plateau has a complex climate system, a unique geographical location, sensitive environmental responses, and a fragile ecosystem, which together give it a distinctive position in global change research. However, uncertainties remain in estimating CO_2 emissions from the agricultural canal-lake continuum within this region. Therefore, this study focused on the agricultural canal-lake Ulansuhai continuum within the Hetao Irrigation District. The objectives were to (1) elucidate the dynamic characteristics of the carbon dioxide flux (F_{CO_2}) in this continuum and its driving factors; and (2) quantify the total CO_2 emission flux ($F_{CO_2 total}$) from both the agricultural ditch system of the Hetao Irrigation District and lakes across the Inner Mongolia Plateau. The findings will provide critical data support for assessing CO_2 emission fluxes from inland waters in a typical agricultural watershed in China.

2. Materials and methods

2.1 Study area

The Hetao Irrigation District in Inner Mongolia (106°10′ to 109° 30′E, 40°10′ to 41°20′N) is located in the arid and semi-arid zone of northwest China. Influenced by the Mongolian high-pressure system, the area experiences strong winds and scarce precipitation. The annual average wind speed ranges from 2.5 m s^{-1} to 3.4 m s^{-1}, and the annual average temperature is between 3.7 °C and 7.6 °C. The soil in the irrigation district is formed from the Yellow River alluvial parent material, primarily consisting of salinized light-colored meadow soil and saline soil. The irrigation district is shaped like a curved fan. Due to its unique natural conditions and geographical location, natural rivers rarely form within this area. Therefore, the runoff in the irrigation district mainly consists of water from the Yellow River system that flows into the intake and drainage canals within the district. With the Ulansuhai Lake serving as the terminal receiving basin, agricultural runoff, industrial wastewater, and domestic sewage from nearly the entire Hetao Irrigation District flow into the lake *via* the Main Drainage Canal, Tongji Canal, Eighth Drainage Canal, Changji Canal, Ninth Drainage Canal, and Tabu Canal[21] (Fig. 1a). The Ulansuhai Lake is elongated in shape, with an average water depth of 0.9 m, reaching a maximum depth of 4 m. Most of the lake area has a water depth between 0.5 and 1.5 m. The total area of the lake is 305.7 km^2, and the open water surface area is 117.5 km^2.[22] It is one of the few shallow lakes located in the arid and semi-arid climatic zones in northern China.[21]

2.2 Sample collection

Between 2023 and 2024, during typical irrigation periods, water samples were collected from 73 sampling points (Fig. 1c) at the surface water layer (0–40 cm) using water samplers, specifically from agricultural canals (C1–C8) and various locations within the Ulansuhai Lake (W1–W5) (Fig. 1b). No extreme weather events occurred during the sampling dates. The water samples were transported to the laboratory under refrigerated conditions for preprocessing and analysis. Water quality parameters such as water temperature (T_W), pH, electrical conductivity (EC), salinity (SA), and dissolved oxygen (DO) were measured *in situ* using a portable water quality analyzer (PONSEL, ODEON, France). The concentrations of total nitrogen (TN) and total phosphorus (TP) in the water samples were determined using a continuous flow analyzer (Alliance Futura, France). Additionally, the total alkalinity of the water samples was measured using the double-indicator titration method. The concentrations of dissolved organic carbon (DOC) and dissolved inorganic carbon (DIC) in the water samples were determined separately using a total organic carbon analyzer (Teledyne Tekmar TOC Torch, USA).

2.3 Calculations of CO_2 partial pressures and fluxes

The P_{CO_2} in water was estimated using the pH-DIC relationship equation:[23,24]

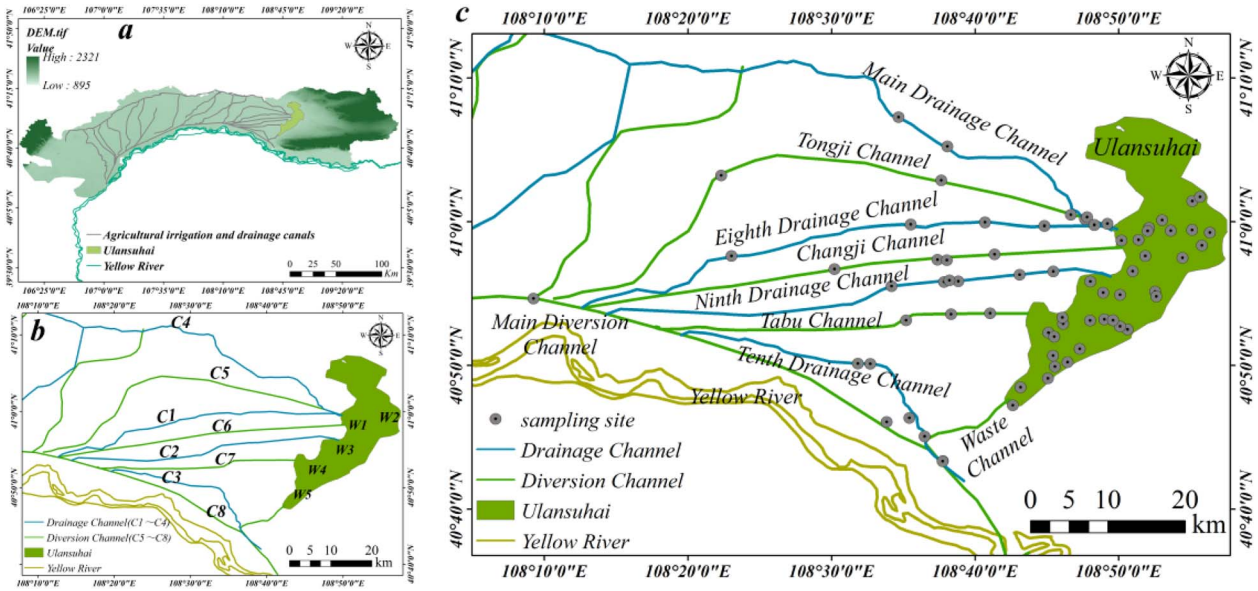

Fig. 1 Agricultural canals-Ulansuhai lake system (a), sampling area (b), and distribution of specific sampling points (c).

$$P_{CO_2} = \frac{[CO_2]}{K_H} = \frac{C_T[H]^2}{\left([H]^2 + [H]^2K_1 + K_1K_2\right)K_H} \quad (1)$$

where C_T represents the concentration of DIC, $[H] = 10^{-pH}$, K_H is the solubility constant, and K_1 and K_2 are the dissociation constants of carbonic acid.[25] They are calculated as follows:

$$PK_0 = -7 \times 10^{-5}T^2 + 0.016T + 1.11 \quad (2)$$

$$PK_1 = 1.1 \times 10^{-4}T^2 - 0.012T + 6.58 \quad (3)$$

$$PK_2 = 9 \times 10^{-5}T^2 + 0.0137T + 10.62 \quad (4)$$

$$\ln K_H = -58.0931 + 90.5069 \times \left(\frac{100}{T_K}\right) + 22.294 \times \ln\left(\frac{T_K}{100}\right) \quad (5)$$

where $PK = -\lg K$, T represents the water temperature in degrees Celsius (°C), and T_K represents the Kelvin temperature of the water (K).

CO_2 flux was quantified only during the non-ice-covered period and estimated using a shallow boundary layer model:[26,27]

$$F_{CO_2} = 0.24 \times (P_W - P_G) \times K \times K_H \quad (6)$$

where the conversion factor is 0.24. F_{CO_2} represents the CO_2 exchange flux per unit area, mmol per m^2 per day. P_w denotes the partial pressure of CO_2 in the surface water, μatm. P_g represents the partial pressure of CO_2 in the atmosphere at water–air equilibrium (400 μatm). K_H is Henry's constant for CO_2, measured in mmol per m^3 per μatm and corrected by using eqn (5). K represents the gas exchange coefficient, cm h^{-1}.

The gas exchange coefficient was calculated by using the following equation:

$$K_{600} = 2.07 + 0.215_{10}^{1.7} \ (V_{10} < 3 \text{ m s}^{-1}) \quad (7)$$

$$K_{600} = 0.72V_{10} \ (V_{10} < 3.7 \text{ m s}^{-1}) \quad (8)$$

$$K_{600} = 0.215V_{10}^2 \ (3 \text{ m s}^{-1} < V_{10} < 15 \text{ m s}^{-1}) \quad (9)$$

$$K_{600} = 0.31V_{10}^2 \ (V_{10} > 3.7 \text{ m s}^{-1}) \quad (10)$$

$$K_{600} = 0.455V_{10}^2 \ (3 \text{ m s}^{-1} < V_{10} < 5\text{m s}^{-1}) \quad (11)$$

$$K_{600} = 0.168 + 0.228V_{10}^{2.2} \ (V_{10} \text{ no requirements}) \quad (12)$$

After calculating the values of K_{600} at different wind speeds, the average is taken as the final K_{600}.

$$K = K_{600} \times \left(\frac{Sc_{(CO_2)}}{600}\right)^X \quad (13)$$

$$Sc_{(CO_2)} = 1911.1 - 118.11t + 3.4527t^2 - 0.04132t^3 \quad (14)$$

where V_{10} represents the wind speed at 10 meters above the water surface, m s^{-1}; $Sc_{(CO_2)}$ denotes the Schmidt number for CO_2 in the surface water; the value of x depends on V_{10}, when $V_{10} < 3.7$ m s^{-1}, $x = -2/3$, and when $V_{10} > 3.7$ m s^{-1}, $x = -1/2$; t represents the temperature of the water, °C.

2.4 Estimation of regional CO_2 emissions

The CO_2 emissions from agricultural canals in the Hetao Irrigation District and lakes across the Inner Mongolia Plateau were estimated by multiplying the respective F_{CO_2} by the number of days during the ice-free period and the total water surface area, as shown in eqn (15).[6,28] The total area of the corresponding lakes in the Inner Mongolia Plateau region ranges from 3625.35 to 4962.06 km^2.[29] We estimated the total water surface area of the canals by multiplying the total length of the canals by their average width. Based on annual temperature data and previous studies, we assumed that the non-ice-

covered period lasts for 150 days. Additionally, due to intermittent drying of agricultural canals during both irrigation and non-irrigation periods, we assumed that these canals have only been storing water for 120 days of the non-ice-covered period.

$$F_{CO_2total} = F_{CO_2} \times SA \times N \times 12 \div 10^{15} \quad (15)$$

where F_{CO_2total} represents the total CO_2 emissions, Tg C per year; F_{CO_2} denotes the CO_2 emission flux per unit area, mmol per m^2 per day; SA stands for the water surface area, m^2; N represents the number of days in the non-ice-covered period, days; 12 is the molar mass of carbon, 12 g mol^{-1}; 10^{15} is the conversion factor from mg to Tg.

2.5 Statistical analyses

Statistical analysis was performed using SPSS 27. First, data normality was verified using the Shapiro–Wilk test. Spearman correlation analysis was employed to examine the correlations among various indicators. Following one-way analysis of variance (ANOVA), Tukey's Honestly Significant Difference (HSD) *post hoc* test was applied for significance testing. Data visualization was conducted using Origin 2022 and ArcMap 10.8. Data presented with the "±" symbol represent the mean ± standard deviation.

3. Results

3.1 Continuum environmental variables

Table 1 systematically presents the spatiotemporal variations of key water environmental parameters within the agricultural ditch-Lake Ulansuhai continuum, including water temperature (T_W), dissolved oxygen (DO), pH, electrical conductivity (EC), salinity (SA), bicarbonate (HCO_3^-) concentration, and total dissolved solids (TDS). The observed variations in these parameters reflected the dynamic hydrogeochemical processes occurring in the continuum.

T_W in agricultural canals (drainage and irrigation canals) was significantly higher than in the lake, with temperature differences reaching up to 3.5 °C during the spring irrigation period and 4.0 °C during the autumn irrigation period. Overall, DO concentrations were higher during the autumn irrigation period and lower during the spring irrigation period. DO levels in the lake area were consistently higher than those in the canals. The overall increase in DO concentration during the autumn irrigation period (33.6% in the lake area and 18.2% in the canals) was associated with the concurrent decrease in water temperature. The pH values across the three water body types within the continuum displayed a distinct alkaline gradient: the highest in the lake (7.8–8.2), followed by irrigation canals (7.5–7.9), and the lowest in drainage canals (7.2–7.6). Lake pH was consistently higher than that in agricultural canals. Furthermore, the pH of all water bodies increased from the spring to the autumn irrigation period. During the spring irrigation period, HCO_3^- concentration in drainage canals (666 ± 175 mg L^{-1}) was significantly higher than that in irrigation canals (326 ± 18 mg L^{-1}) and that in the lake (482 ± 112 mg L^{-1}), confirming that the drainage system acted as a key conduit for regional salt transport. HCO_3^- concentrations decreased significantly during the autumn irrigation period, with mean values of 206 ± 51 mg L^{-1} (lake), 338 ± 149 mg L^{-1} (drainage

Table 1 Dynamic variations of physicochemical parameters for different water types in the continuum across hydrological periods

		Period	
Types	Parameter	Spring irrigation	Autumn irrigation
Ulansuhai (W1–W5)	T_W (°C)	20.1 ± 0.3	11.4 ± 0.7
	DO (mg L^{-1})	6.39 ± 1.36	8.54 ± 0.86
	pH	8.21 ± 0.20	8.77 ± 0.36
	EC (mS cm^{-1})	2.61 ± 1.33	2.81 ± 1.15
	SA (g kg^{-1})	1.46 ± 0.27	1.53 ± 0.55
	HCO_3^-(mg L^{-1})	482 ± 112	206 ± 51
	TDS (ppm)	1557 ± 316	1558 ± 649
Drainage canal (C1–C4)	T_W (°C)	23.6 ± 1.1	15.4 ± 1.8
	DO (mg L^{-1})	6.59 ± 1.56	7.79 ± 0.72
	pH	7.83 ± 0.60	8.07 ± 0.49
	EC (mS cm^{-1})	10.83 ± 7.14	3.06 ± 2.27
	SA (g kg^{-1})	6.45 ± 5.07	3.36 ± 2.85
	HCO_3^- (mg L^{-1})	666 ± 175	338 ± 149
	TDS (ppm)	5681 ± 3385	3316 ± 2828
Diversion canal (C5–C8)	T_W (°C)	22.2 ± 0.9	15.0 ± 1.5
	DO (mg L^{-1})	6.78 ± 0.25	7.55 ± 0.31
	pH	8.00 ± 0.38	8.17 ± 0.24
	EC (mS cm^{-1})	0.96 ± 0.48	1.19 ± 1.10
	SA (g kg^{-1})	0.42 ± 0.037	0.84 ± 0.0.81
	HCO_3^- (mg L^{-1})	326 ± 18	243 ± 83
	TDS (ppm)	400 ± 35	661 ± 653

canals), and 243 ± 83 mg L^{-1} (irrigation canals). Parameters EC (>1 mS cm^{-1}), SA (0.37–13.57 g kg^{-1}), and TDS (359–9999 ppm) exhibited consistent trends, following the pattern: drainage canals > lake > irrigation canals.

3.2 Spatiotemporal variation characteristics of TN, TP, and dissolved carbon within the continuum

During the spring irrigation period, the mean TP concentrations in lakes, drainage canals, and diversion canals were 0.16 ± 0.0095 mg L^{-1}, 0.0095 ± 0.0067 mg L^{-1}, and 0.0071 ± 0.0096 mg L^{-1}, respectively. During the autumn irrigation period, the mean concentrations were 0.023 ± 0.0075 mg L^{-1}, 0.026 ± 0.0095 mg L^{-1}, and 0.018 ± 0.0090 mg L^{-1}, respectively. Across both irrigation periods, lakes consistently had relatively high TP concentrations, diversion canals had relatively low concentrations, and drainage canals had intermediate concentrations (Fig. 2a). For TN, during the spring irrigation period, the mean TN concentrations in lakes, drainage canals, and diversion canals were 0.42 ± 0.16 mg L^{-1}, 0.70 ± 0.44 mg L^{-1}, and 1.79 ± 0.16 mg L^{-1}, respectively. During the autumn irrigation period, the mean concentrations were 1.09 ± 0.12 mg L^{-1}, 1.83 ± 0.72 mg L^{-1}, and 1.88 ± 0.40 mg L^{-1}, respectively. Within each irrigation period, diversion canals had the highest TN concentrations, lakes had the lowest, and drainage canals had intermediate concentrations (Fig. 2b).

The spatiotemporal variation characteristics of dissolved carbon in the agricultural canals and lakes within the continuum are shown in Fig. 2c. Overall, the content of DIC in the continuum was significantly higher than that of DOC, and the two exhibited a significant positive correlation ($R^2 = 0.75$; $p < 0.001$) (Fig. 2d). Both DOC and DIC concentrations displayed distinct seasonal differences across the continuum. Concentrations during the spring irrigation period were significantly higher than during the autumn irrigation period, reaching 1.4–2.1 times the levels observed in autumn. The average concentrations of DOC and DIC in Lake Ulansuhai (35.16 ± 15.99 mg L^{-1} and 60.07 ± 11.53 mg L^{-1}, respectively) were significantly higher than the averages reported for freshwater lakes in China (5.80 mg L^{-1} and 29.38 mg L^{-1}). The average DOC concentration (23.92 ± 14.71 mg L^{-1}) in agricultural canals was lower than in Lake Ulansuhai (35.16 ± 15.99 mg L^{-1}), while their average DIC concentration (70.55 ± 32.29 mg L^{-1}) was higher than in the lake (60.07 ± 11.53 mg L^{-1}). The spatial distribution pattern revealed that DOC and DIC concentrations in the northern inflow zone of Lake Ulansuhai were higher than those in the southern drainage zone. Within the agricultural canals, the highest concentrations of DOC and DIC were found in the Eighth Drainage canal, Ninth Drainage canal, and Tenth Drainage canal.

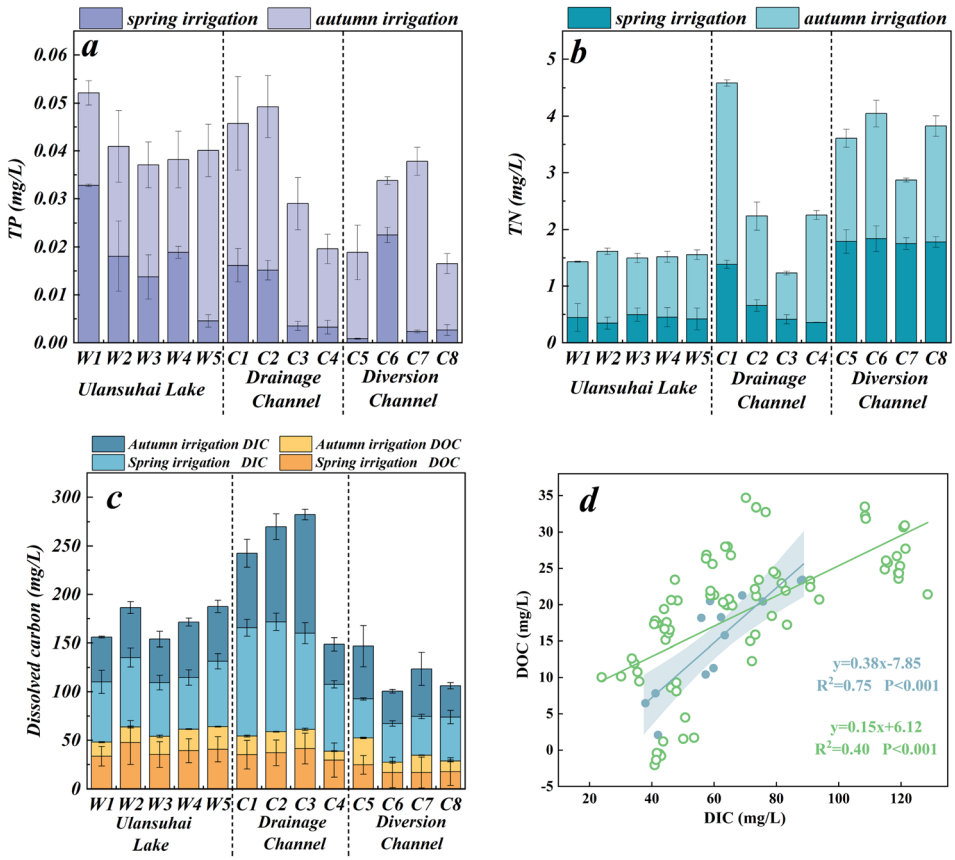

Fig. 2 Spatiotemporal variations of total phosphorus (TP) (a), total nitrogen (TN) (b), and dissolved carbon in the agricultural ditch-lake continuum (c); and the correlation between DIC and DOC (blue dots in (d) represent the continuous system's average values; green dots represent all data).

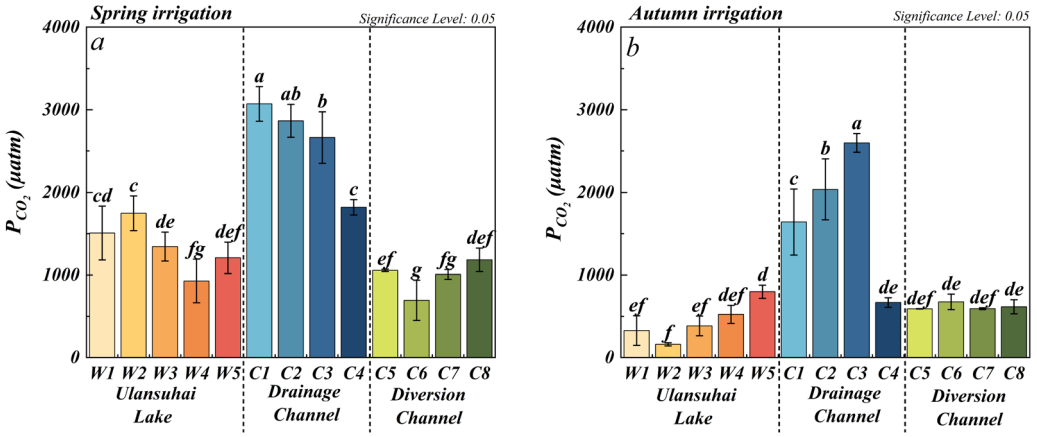

Fig. 3 Partial pressure of carbon dioxide (P_{CO_2}) during the spring irrigation period (a) and autumn irrigation period (b) in the continuum.

3.3 Spatiotemporal variations in P_{CO_2} and F_{CO_2} within the continuum

During the irrigation periods, there were significant differences in P_{CO_2} among lakes and different types of canals ($p < 0.05$). The P_{CO_2} in lakes ranged from 701 μatm to 1981 μatm, with an average of 1346 ± 360 μatm. In agricultural canals, P_{CO_2} varied between 525 μatm and 3366 μatm, with an average of 1538 ± 887 μatm. The P_{CO_2} in canals was significantly higher than the atmospheric average (400 μatm) during both irrigation periods. However, P_{CO_2} in the Ulansuhai Lake was undersaturated during the autumn irrigation period. Overall, P_{CO_2} in both canals and lake waters was higher during the spring irrigation period than during the autumn irrigation period, with higher P_{CO_2} in agricultural canals than in lakes (Fig. 3).

Regarding the area-based F_{CO_2}, during the spring irrigation period, the F_{CO_2} in lakes ranged from 14.33 mmol per m^2 per day to 72.51 mmol per m^2 per day, with an average of 43.85 ± 16.30 mmol per m^2 per day. In drainage canals, F_{CO_2} varied between 56.07 mmol per m^2 per day and 121.05 mmol per m^2 per day, averaging 93.63 ± 22.13 mmol per m^2 per day. For diversion canals, F_{CO_2} ranged from 5.76 mmol per m^2 per day to 43.15 mmol per m^2 per day, with an average of 25.41 ± 9.61 mmol per m^2 per day (Fig. 4a). The F_{CO_2} values were all greater than 0, showing a trend of drainage canals > lakes > diversion canals. During the autumn irrigation period, the F_{CO_2} in lakes ranged from −11.50 mmol per m^2 per day to 18.27 mmol per m^2 per day, with an average of −0.69 ± 11.89 mmol per m^2 per day. In drainage canals, F_{CO_2} varied between 7.60 mmol per m^2 per day and 97.70 mmol per m^2 per day, averaging 46.09 ± 34.42 mmol per m^2 per day. For diversion canals, F_{CO_2} ranged from 5.12 mmol per m^2 per day to 53.95 mmol per m^2 per day, with an average of 18.68 ± 16.47 mmol per m^2 per day (Fig. 4b). During the autumn irrigation period, the F_{CO_2} in agricultural canals was greater than 0, showing a trend of drainage canals > irrigation canals, indicating CO_2 emissions to the atmosphere. However, in the Ulansuhai Lake, negative F_{CO_2} values were observed (Fig. 4b). Overall, there were significant differences in F_{CO_2} among different types of water bodies ($p < 0.05$) (Fig. 4). F_{CO_2} during the spring irrigation period was higher than that during the autumn irrigation period, and the area-based F_{CO_2} observed in canals was higher than in lakes, indicating widespread and persistent emissions of CO_2 to the atmosphere.

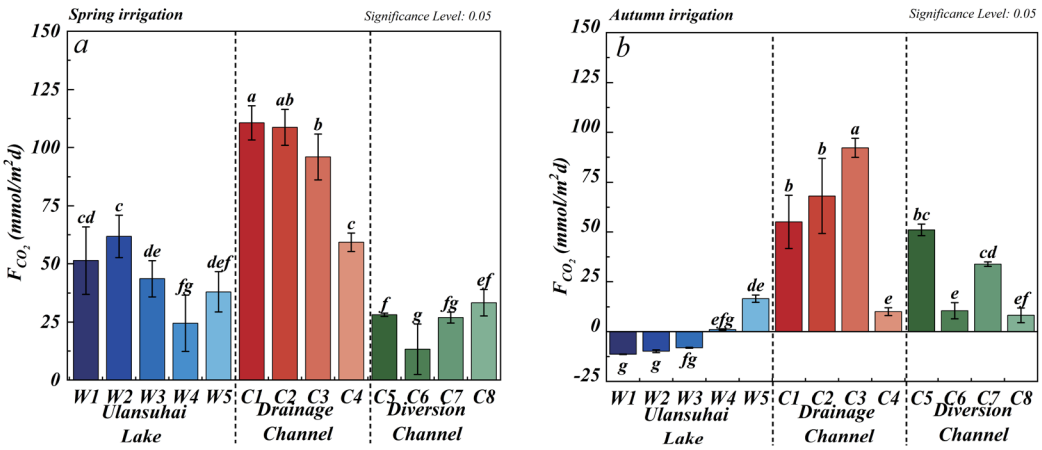

Fig. 4 CO_2 flux (F_{CO_2}) during the spring irrigation period (a) and autumn irrigation period (b) in the continuum.

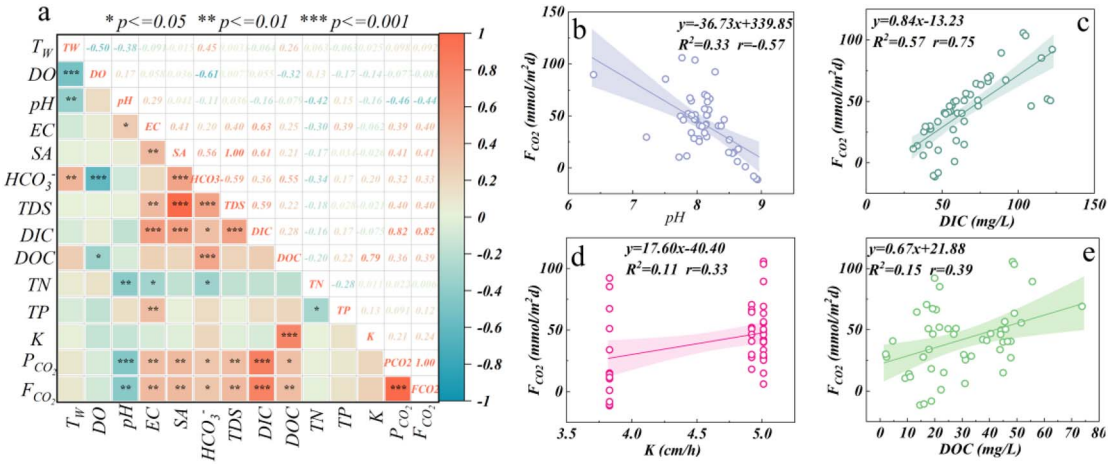

Fig. 5 Correlation analysis of F_{CO_2} during the ice-free period in the continuum. (a) Correlation heatmap between F_{CO_2} and environmental factors; (b)–(e) represent the correlation analysis between F_{CO_2} and each major environmental factor, respectively.

3.4 Driving factors influencing CO_2 emissions in the continuum

When the P_{CO_2} in water exceeds the atmospheric equilibrium value, CO_2 is emitted at the water–air interface. F_{CO_2} is negatively correlated with pH ($R^2 = 0.33$, $p < 0.001$) (Fig. 5b), positively correlated with DIC ($R^2 = 0.57$, $p < 0.001$) (Fig. 5c), and positively correlated with HCO_3^- ($p < 0.05$) (Fig. 5a). It is also positively correlated with DOC ($R^2 = 0.15$, $p < 0.01$) (Fig. 5e), potassium (K) ($R^2 = 0.11$, $p < 0.05$) (Fig. 5d), EC, and SA ($p < 0.01$) (Fig. 5a). These environmental factors jointly regulate F_{CO_2} in the continuum.

3.5 Regional CO_2 emissions from the continuum and lakes across the Inner Mongolia Plateau

Agricultural canals are ubiquitous in global agricultural regions, covering up to 7% of drained croplands and serving as a significant source of greenhouse gas emissions. In the Hetao Irrigation District of Inner Mongolia, various types of canals and Lake Ulansuhai constitute important greenhouse gas sources (Fig. 4). The total CO_2 emissions from the entire continuum reached approximately 0.023 Tg C per year. Lake Ulansuhai alone contributed 0.013 Tg C per year, accounting for 57% of the continuum's total emissions. Agricultural canals emitted 0.0097 Tg C per year (43% of the continuum), with drainage canals (0.0054 Tg C per year) exhibiting higher emissions than irrigation canals (0.0043 Tg C per year) (Fig. 6a). For context, lakes across the Inner Mongolia Plateau emitted 0.22 Tg C per year, representing about 2.6% of China's total lake CO_2 emissions. This emission level was lower than those from lake systems in Northeast China, Northwest China, the Yangtze River Basin, the Huang-Huai-Hai Plain, and the Tibetan Plateau region (Fig. 6b).

4. Discussion

4.1 Physicochemical factors affecting CO_2 emissions in the continuum

The solubility pump and the biological pump jointly influence the CO_2 exchange rate at the water–air interface.[30] The solubility

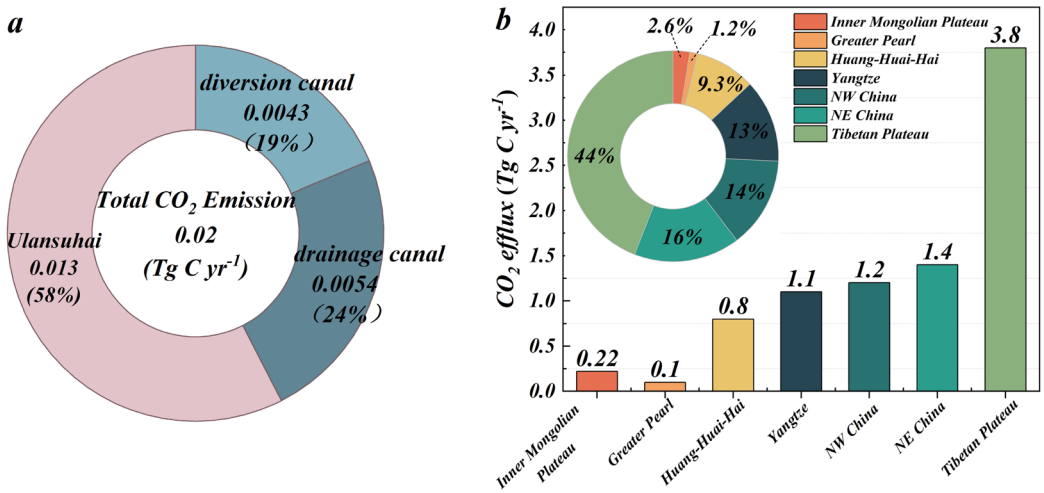

Fig. 6 Total CO_2 emissions in (a) the watershed continuum and (b) Inner Mongolian Plateau lakes.

pump is influenced by factors such as wind speed, water temperature, alkalinity, and carbonate decomposition.[31] In contrast, the biological pump primarily relies on the photosynthesis and respiration of aquatic organisms, especially phytoplankton.[32]

Aquatic CO_2 flux is influenced by multiple factors, exhibiting high complexity and variability.[33] In aquatic ecosystems, DIC is the sum of inorganic carbon species (HCO_3^-, H_2CO_3, CO_3^{2-}, and CO_{2aq}), and the balance among these components depends on temperature and pH. In this continuum, with a pH range of 7.51 to 8.94, DIC is dominated by HCO_3^-.[34] Driven by intense soil erosion and chemical weathering in the Yellow River basin, the carbonate system composed of DIC and water pH is one of the factors controlling the high P_{CO_2} in the water bodies of this continuum.[34] F_{CO_2} is negatively correlated with pH ($R^2 = 0.33$, $p < 0.001$) (Fig. 5b) and positively correlated with DIC ($R^2 = 0.57$, $p < 0.001$) (Fig. 5c). Changes in pH disrupt the carbonate reaction equilibrium, thereby affecting the P_{CO_2} of the water body and the F_{CO_2} at the water–air interface, which alters the amount of CO_2 efflux. The pH level is negatively correlated with both P_{CO_2} and F_{CO_2} (Fig. 5a), indicating the importance of the carbonate buffer as a source and sink of CO_2.[35] The study by Zhou *et al.*[5] reveals a significant negative exponential relationship between river F_{CO_2} and pH. The primary reason behind this phenomenon is that pH regulates the carbonate balance in water, thereby affecting the CO_2 partial pressure and CO_2 emissions of water. Under the action of the "biological carbon pump", aquatic organisms fix inorganic carbon into organic carbon, resulting in the burial of some carbon, which reduces the DIC concentration in the water body, leading to a decrease in water CO_2 concentration and subsequently a decrease in F_{CO_2}. Conversely, when DIC concentration increases, it causes more CO_2 to escape from the water body. The HCO_3^- produced by the dissolution of carbonate rocks by H_2CO_3 also causes an increase in P_{CO_2} and F_{CO_2}. In the weakly alkaline continuum, the high concentration of HCO_3^- forms a buffering system. When water temperature increases, pH fluctuates, or water–air disturbance intensifies, and the carbonate equilibrium shifts to the right: $2HCO_3^- \rightleftharpoons CO_3^{2-} + CO_2\uparrow + H_2O$, resulting in CO_2 degassing. Therefore, carbonate weathering indirectly promotes an increase in P_{CO_2} and CO_2 emission by supplying HCO_3^-, rather than directly producing CO_2. This mechanism is particularly pronounced in the high-DIC, high-pH water bodies of the study region.

The sources and transformation processes of DIC significantly influence CO_2 emissions. Exogenously input DIC directly affects the P_{CO_2} in water bodies, often leading to a supersaturated state of CO_2. This supersaturation subsequently drives the release of CO_2 into the atmosphere.[36–38] For example, research in Lake Taihu has shown that in areas dominated by exogenous inputs of DIC and DOC, the P_{CO_2} at estuaries can reach twice that in open water areas. This phenomenon primarily stems from high-intensity exogenous carbon inputs.[24] Our recent study confirms that the DIC in the agricultural canal-lake water system of the Hetao Irrigation District originates mainly from exogenous inputs.[34] After entering the water body, this DIC may undergo a series of biogeochemical processes, such as photosynthesis-respiration and carbonate precipitation/dissolution. These processes not only alter the concentration and composition of DIC but also affect the water's pH, thereby indirectly influencing F_{CO_2}. Similarly, Lv *et al.*[39] also found a significant positive correlation between F_{CO_2} and alkalinity-DIC in the Nihe Reservoir.

Furthermore, F_{CO_2} is positively correlated with K ($R^2 = 0.11$, $p < 0.05$) (Fig. 5d). CO_2 emissions depend on the water body's P_{CO_2} and the gas transfer velocity K. P_{CO_2} influences the direction of CO_2 diffusion at the water–air interface, thereby controlling the carbon emission rate. F_{CO_2} exhibits significant spatiotemporal variability. The Inner Mongolia Plateau has a flat terrain, allowing cold front winds and cyclonic winds to flow freely, resulting in a high annual average wind speed. High wind speeds can reduce the thickness of the water boundary layer, thereby increasing the diffusion rate of carbon in surface waters. When K increases, surface water disturbance intensifies, leading to an increase in the gas exchange interface area between the water and the atmosphere, which facilitates the escape of CO_2 from the water body into the atmosphere.[11,40,41]

4.2 The impact of human activities on CO_2 emissions in the continuum

Anthropogenic-induced changes in the water balance will lead to alterations in carbon storage and carbon flux within the watershed, with changes in vegetation cover and irrigation playing significant roles in regulating the carbon cycle. The widespread adoption of agricultural activities and chemical fertilizers, coupled with irrigation drainage, conveys substantial agricultural pollutants (livestock manure) and nutrients (*e.g.*, nitrogen and phosphorus) into water bodies within agricultural watersheds.[6,11,42] This process provides sufficient substrates for CO_2 production, thereby establishing agricultural irrigation-drainage channels as carbon emission hotspots.[20,43–45] DOC from terrestrial sources to aquatic environments constitutes a significant external input pathway of organic carbon into freshwater ecosystems. Simultaneously, it represents a key process releasing CO_2 to the atmosphere. The load of external DOC input regulates the dynamic changes in aquatic CO_2 emissions by acting as a substrate for microbial metabolism. Elevated DOC concentrations provide abundant organic carbon substrates to the water body. This imported DOC can undergo photodegradation and is subsequently degraded by aquatic microorganisms, such as bacteria and phytoplankton. Within lake systems, DOC is typically the organic carbon component most readily mineralized and converted into CO_2. This process significantly influences dissolved CO_2 concentrations and their subsequent flux to the atmosphere.[46] Further supporting this mechanism, research by Zhou *et al.*[5] found significant positive correlations between riverine F_{CO_2} and concentrations of Total Organic Carbon (TOC), DOC, and TN. Similarly, this study also observed a positive correlation between aquatic P_{CO_2} and DOC ($p < 0.05$) (Fig. 5a), and between F_{CO_2} and DOC ($p < 0.01$) (Fig. 5e). Collectively, this evidence indicates that DOC decomposition is a key driver of aquatic CO_2 emissions. Substantial inputs of organic matter and agricultural practices lead to excessive nutrient loads entering the aquatic continuum. Concurrently,

Table 2 F_{CO_2} in major rivers and lakes in China[a]

Basin name	F_{CO_2} (mmol per m^2 per day)	References
Hongze Lake	−17.3–310.29 (43.5 ± 63.5)	57
Chaohu Lake	5.61 ± 6.35	58
Dongting Lake	−12.97	59
Poyang Lake	19.49	59
Baiyangdian Lake	−16.19–623.54 (25.52 ± 3.60)	60
Dianchi Lake	−9.79	59
Taihu Lake	−23.6–808.1 (18.2 ± 8.4)	24
Qinghai Lake	1.29	61
Ulansuhai Lake	35.99	This study
Global saline lakes	81–105 (80)	26
China's lakes	−35.56–111.6 (38.05)	62
Global lakes	28.8	63
Global artificial reservoirs	41.5	64
Hetao Irrigation District	47.91	This study
Songhua River	255.3	28 and 43
Liao River	362.6	28 and 43
Hai River	47.5	43
Yellow River	855.8	43 and 65
Huai River	515.7	28 and 43
Yangtze River	38.9	43 and 66
Yarlung Zangbo River	180.3	28 and 43
Pearl River	158.9	28 and 43
All rivers	384	28 and 43

[a] DLC, QHL, CHL, PYL, TL, DTL, ULS, HZL, and BYD represent the Dianchi Lake, Qinghai Lake, Chaohu Lake, Poyang Lake, Taihu Lake, Dongting Lake, Ulansuhai Lake, Hongze Lake, and Baiyangdian Lake. HID, HHR, PR, YZR, SHR, LHR, HR, YR, and CJ represent agricultural canals in the Hetao Irrigation District, Haihe River, Pearl River, Yarlung Zangbo River, Songhua River, Liaohe River, Huaihe River, Yellow River, and Yangtze River.

ditch systems are characterized by high nutrient levels, low flow rates, and active biogeochemical interactions between nutrients. These conditions may enhance carbon transformation and emission processes.[11] Additionally, salinity (typically measured as electrical conductivity) exerts a particularly significant influence. High salinity itself can promote the diffusive flux of CO_2. Agricultural drainage and regional soil characteristics lead to elevated salt and alkali content in ditch water. Furthermore, substantial external inputs contribute not only salts but also abundant organic matter. This increased organic matter directly provides a carbon source through decomposition or mineralization processes, significantly stimulating CO_2 production and emission.[26] The data from this study indicate a positive correlation between F_{CO_2} and SA ($p < 0.001$) (Fig. 5a). High salinity may promote the anaerobic decomposition of organic matter and subsequent CO_2 production by inhibiting the activity of nitrifying bacteria. Under alkaline conditions (pH > 8), the chemical degradation of organic matter is accelerated. Simultaneously, these conditions promote the reaction between CO_2 and OH^- to form HCO_3^-, establishing a dynamic equilibrium system involving CO_2–HCO_3^-–CO_3^{2-}.[47,48]

4.3 Agricultural canals and lakes in high-latitude regions are hotspots for CO_2 emissions

Both natural and human-made inland waters are often affected by intermittent droughts. Such ecosystems may temporarily dry up partially or completely, and in some cases, they may even dry up permanently.[49] The irrigation-drainage channels in the Hetao Irrigation District of Inner Mongolia, which experience temporary drying up after irrigation periods, are characteristically intermittent agricultural canals. During the sampling period, they were supersaturated and served as sources of CO_2 emissions throughout the year. The total annual CO_2 emissions amounted to 0.0097 Tg C per year. Their average F_{CO_2} (49.43 ± 37.30 mmol per m^2 per day) was much lower than the average F_{CO_2} of rivers in China (384 mmol per m^2 per day) and also lower than those of China's major rivers (Yangtze River, Yellow River, Huai River, Liao River, Songhua River, Yarlung Zangbo River, and Pearl River) (Table 2 and Fig. 7). However, this value was higher than the average F_{CO_2} of lakes (standing waters) in China (38.05 mmol per m^2 per day) (Table 2). Field observations revealed significantly higher F_{CO_2} in agricultural canals than that in the Ulansuhai Lake, likely attributable to fertilizer application and organic matter decomposition within the soil-vegetation system. Concurrently, irrigation activities enhance

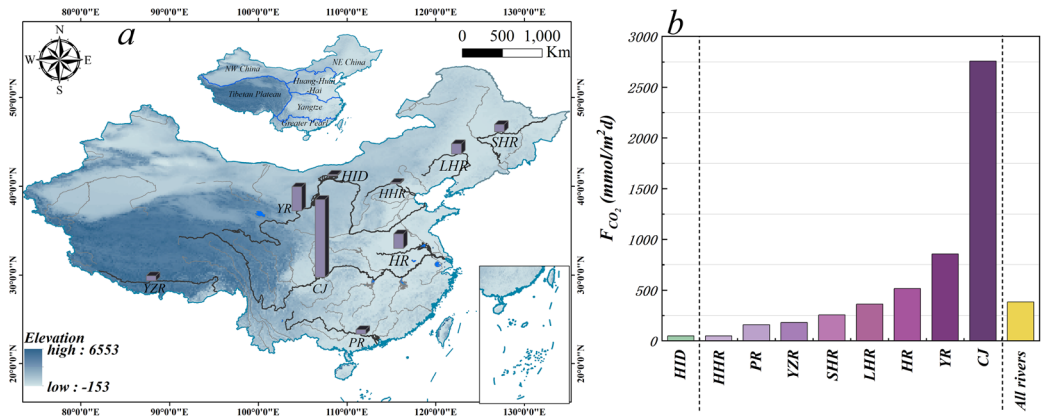

Fig. 7 Spatial characteristics of F_{CO_2} in major Chinese rivers (a) and changes in FCO_2 emission flux per unit area (b). (HID, HHR, PR, YZR, SHR, LHR, HR, YR, and CJ represent agricultural canals in the Hetao Irrigation District, Hai River, Pearl River, Yarlung Zangbo River, Songhua River, Liao River, Huai River, Yellow River, and Yangtze River. "All rivers" represents the average F_{CO_2} value of rivers in China).

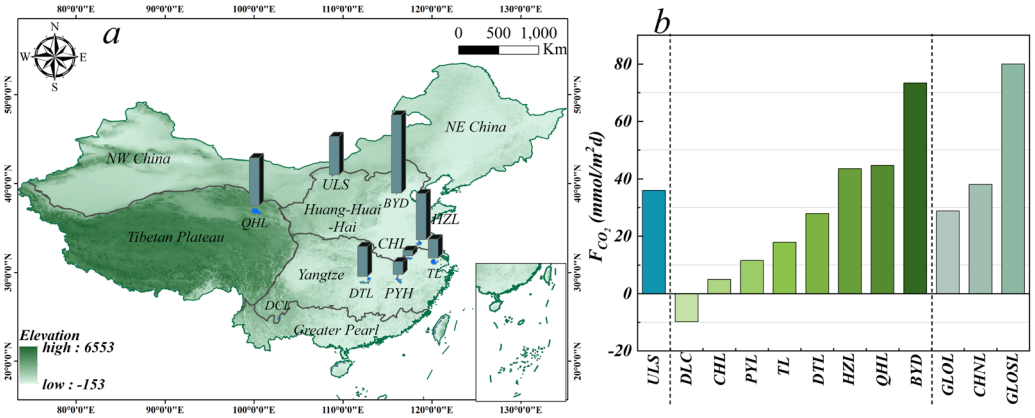

Fig. 8 Spatial characteristics of F_{CO_2} in major Chinese lakes (a) and changes in F_{CO_2} emission flux per unit area (b). (DLC, QHL, CHL, PYL, TL, DTL, ULS, HZL, and BYD represent, respectively, Dianchi Lake, Qinghai Lake, Chaohu Lake, Poyang Lake, Taihu Lake, Dongting Lake, Ulansuhai Lake, Hongze Lake, and Baiyangdian Lake. GLOL represents the average F_{CO_2} value of global lakes, CHNL represents the average F_{CO_2} value of lakes in China, and GLOSL represents the average F_{CO_2} value of global salt lakes).

hydrological connectivity across the aquatic continuum, facilitating increased inputs of terrestrial carbon and dissolved CO_2 into ditch networks.[44,45] Previous research conducted in the western Chengdu Plain-a vital agricultural region in southwestern China-further demonstrated that rice-cultivation ditch systems in this area persistently utilize traditional agricultural amendments (*e.g.*, chemical fertilizers, fungal residues, and manure). This agricultural practice constitutes a key contributing factor to elevated carbon emissions.[11]

The average F_{CO_2} of the Ulansuhai Lake (29.68 ± 25.69 mmol per m^2 per day) was slightly higher than that of China's major freshwater lakes (Taihu Lake, Chaohu Lake, Poyang Lake, Dongting Lake, and Dianchi Lake) and was comparable to the average global lake emissions (28.8 mmol per m^2 per day) and the average emissions of lakes in China (38.05 mmol per m^2 per day) (Fig. 8 and Table 2). During the observation period, the total annual CO_2 emissions from the Ulansuhai Lake amounted to 0.013 Tg C per year. The Ulansuhai Lake has a relatively small area (293 km^2) and shallow water, which results in weak stratification of temperature and dissolved oxygen. This promotes aerobic respiration in the bottom water and sediments, thereby increasing CO_2 production. The study by Zhou *et al.*[5] indicates that most of the high F_{CO_2} values in lake systems occur in lakes with a water surface area of less than 400 km^2, while extremely high F_{CO_2} values are found in lakes with a water surface area of less than 10 km^2. Existing studies have confirmed significant positive correlations between CO_2 concentrations in freshwater ecosystems and both the proportion of cultivated land and agricultural intensity within watersheds. Agricultural activities enhance the input efficiency of organic matter and nutrients into aquatic systems, potentially activating microbial metabolic processes that drive CO_2 production.[7,8,50] Agriculture occupies a significant portion of the global ice-free land surface.[7] In the context of greenhouse gas emission research, agricultural canals remain the least understood type of waterways.[6] As the world's second-largest irrigated agricultural country, China's multi-level artificial ditch system holds typical research value due to its complexity.[11] Therefore, there is an urgent need to quantify CO_2 emissions from agricultural canal-lake systems in typical regions, deepen the understanding of their regulating environmental factors, and improve the monitoring frequency of greenhouse gases.[49]

From a spatial perspective, the F_{CO_2} of natural rivers in China decreases from the south to the north (Fig. 7a), with high values occurring in the Yangtze River basin. High F_{CO_2} values for lakes in China are concentrated mainly in the Qinghai-Tibet Plateau and the Huang-Huai-Hai region, while low values are mainly distributed in the eastern lake regions. The F_{CO_2} levels of rivers and lakes in high-latitude regions are higher than those in the eastern and Yunnan-Guizhou lake regions (Fig. 8a). The typical characteristics of lakes in Inner Mongolia include relatively small areas, shallow water depths, and severe salinization pollution. Lakes on the Inner Mongolia Plateau are generally characterized by relatively small surface areas, shallow water depths (with an average depth ranging from 0.4 to 1.1 m), water quality ranging from fresh to brackish, and severe salinization. The total CO_2 emissions from these lakes are estimated at approximately 0.22 Tg C per year, which is higher than that of the Pearl River Basin, comparable to that of the Huang-Huai-Hai Basin, but considerably lower than those of the Yangtze River Basin, and the northwestern, northeastern, and Qinghai-Tibet Plateau regions (Fig. 6b). The main factors contributing to these differences include (1) the Inner Mongolia Plateau experiences low annual mean temperatures and a long ice-covered period. Low temperatures limit primary productivity, while the ice-covered period promotes the accumulation of organic matter, which subsequently forms carbon metabolism hotspots after ice breakup. High-latitude lakes generally exhibit high CO_2 fluxes.[18] Shallow lakes on the Inner Mongolia Plateau follow this pattern, whereas lakes on the Qinghai-Tibet Plateau, despite being cold, are larger in area and have higher salinity, leading to different driving mechanisms. (2) Lakes on the Inner Mongolia Plateau have high salt and alkali contents. High salinity may inhibit nitrifying bacterial activity and thereby promote anaerobic decomposition of organic matter and CO_2 production. Alkaline conditions (pH > 8) accelerate chemical degradation of

organic matter and shift the CO_2–HCO_3^-–CO_3^{2-} equilibrium, affecting CO_2 emission. In contrast, lakes in eastern and southern China are mostly neutral to weakly acidic, and their carbonate system behavior differs. (3) The water bodies of Inner Mongolian lakes are shallow, resulting in weak thermal and oxygen stratification, which enhances aerobic respiration in bottom water and sediments and thus increases CO_2 production (characteristics and influencing factors of CO_2 emission from inland waters in China). Large eastern lakes (*e.g.*, Lake Taihu and Lake Poyang) are deep and expansive; stratification and hypoxic zones there mainly affect CH_4 emissions, with different patterns of CO_2 contribution. (4) The intensity of agricultural fertilization and irrigation around Inner Mongolian lakes is lower than that in the eastern lake region. Intense human activities in the eastern region cause widespread eutrophication, leading to massive algal blooms; the resulting high photosynthetic uptake of CO_2 reduces the average F_{CO_2}.

4.4 Uncertainty in the estimation of P_{CO_2} and F_{CO_2}

In waters with high conductivity and high pH, HCO_3^- contributes the primary portion of the total alkalinity. In such hard waters, dissolved CO_2 constitutes only a minor fraction of DIC compared to HCO_3^-. P_{CO_2} can be calculated using the dissociation constants of carbonic acid (as a function of temperature) and either of the paired measurements: pH–total alkalinity or pH–DIC. However, organic acid anions within DOC may contribute significantly to alkalinity in some water bodies, particularly those that are acidic, poorly buffered, and organic-rich. In these cases, P_{CO_2} calculated based on pH and alkalinity will be significantly overestimated.[51] This overestimation primarily stems from the contribution of organic acids to alkalinity as well as the reduction in the buffering capacity of the carbonate system under low pH conditions.[51] Furthermore, in alkaline rivers, 53% of the measured alkalinity values were below 0.07 meq L^{-1}, resulting in substantial uncertainty in alkalinity-based CO_2 quantification.[52] Variations in pH measurement precision are typically the primary driver of discrepancies between measured and calculated P_{CO_2}. In this study, the pH values at all sampling sites exceeded 7 (Table 1), and DOC concentrations were low (Fig. 2). These conditions indicate that the contribution of organic acids to alkalinity and the consequent overestimation of calculated P_{CO_2} are likely to have minimal impact within the context of this study.[51] Previous research has also shown a strong correlation between P_{CO_2} values calculated based on pH and DIC and those measured using the headspace equilibration method.[53] Similar findings have also been reported in studies on the Hudson River.[54] Estimates of F_{CO_2} likewise carry uncertainty. This study employed a wind speed-based model to calculate F_{CO_2}. However, the gas transfer velocity (K) is influenced by multiple factors (*e.g.*, wind speed, boundary layer stability, surfactants, and bubble-mediated transfer), and k values derived from different methods exhibit variation. Consequently, approaches relying solely on wind speed to predict gas transfer velocity have inherent limitations.[55] Nevertheless, gas transfer velocity is primarily governed by wind-driven turbulence at the air–water interface.[56] Consequently, this study still estimated k based on its relationship with wind speed, specifically adopting a parameterization approach that links the normalized gas transfer velocity (K_{600}) to environmental drivers such as wind speed. Specifically, K_{600} values were calculated under six distinct wind speed conditions, and their average was adopted as the final K_{600} value.

5. Conclusion

Agricultural irrigation/drainage canals and lakes in high-latitude regions are hotspots for greenhouse gas emissions. However, their carbon evasion processes remain understudied and urgently need to be quantified and incorporated into the global carbon budget. This study reveals the dynamic characteristics of CO_2 emissions in a typical agricultural irrigation water system-lake continuum in cold and arid regions of northern China. The average F_{CO_2} in drainage canals was higher than that in irrigation canals. The average F_{CO_2} from agricultural canals was significantly higher than that from the connected Lake Ulansuhai and the average level of Chinese lakes, but lower than that of major Chinese rivers. The average F_{CO_2} of Lake Ulansuhai was comparable to the average level of Chinese lakes, with local net CO_2 uptake occurring during the autumn irrigation period. CO_2 emissions were jointly regulated by the physicochemical properties of the water bodies and anthropogenic activities (*e.g.*, fertilization and irrigation). The estimated annual CO_2 emissions from agricultural canals in the irrigation district and lakes on the Inner Mongolia Plateau were 0.0097 Tg C per year and 0.22 Tg C per year, respectively, which were comparable to the carbon emissions from the Huang-Huai-Hai River Basin in China. This study provides fundamental data for carbon cycle research in cold and arid regions and offers a scientific basis for the management of salinization and eutrophication, and the protection of the water environment of the Yellow River.

Author contributions

Ying Wang: writing – original draft, visualization, formal analysis, methodology, investigation. Wenzhu Yang: writing – review & editing. Yan Jiao: writing – review & editing, conceptualization.

Conflicts of interest

The authors declare no known competing financial interests or personal relationships that could influence the results reported in this study.

Data availability

All data from this study are included in the article. The datasets are also available from the corresponding author upon reasonable request.

Acknowledgements

We sincerely acknowledge all colleagues who participated in field investigations and data collection and analysis, and contributed to this research. This work was supported by the National Natural Science Foundation of China (Grant No. U25A20789; 42265004), The Science Foundation (A) for Young Scholars from Natural Science Foundation of Inner Mongolia Autonomous Region of China (2026QAYX004), the Program for Young Talents in Science and Technology at Universities of Inner Mongolia Autonomous Region (NJYT23041), the Key Research & Development and Achievement Transformation Plan of Inner Mongolia Autonomous Region (2025KJHZ0017), and the Natural Science Foundation of Inner Mongolia Autonomous Region (Grant No. 2024MS04026).

References

1 Y. Gao, J. J. Li, S. Y. Wang, J. J. Jia, F. Wu and G. R. Yu, Global inland water greenhouse gas (GHG) geographical patterns and escape mechanisms under different water level, *Water Res.*, 2025, **269**, 122808.

2 Y. Gao, J. J. Jia, Y. Lu, K. Sun, J. Wang and S. Y. Wang, Carbon transportation, transformation, and sedimentation processes at the land-river-estuary continuum, *Fundam. Res.*, 2022, **4**(6), 1594–1602.

3 T. J. Battin, R. Lauerwald, E. S. Bernhardt, E. Bertuzzo, L. Gómez Gener and R. O. Hall, River ecosystem metabolism and carbon biogeochemistry in a changing world, *Nature*, 2023, **613**(7944), 449–459.

4 S. Li, X. X. Lu and R. T. Bush, CO_2 partial pressure and CO_2 emission in the Lower Mekong River, *J. Hydrol.*, 2013, **504**, 40–56.

5 T. Zhou, X. Wang, Z. Xiao, Z. Qing, X. Li, J. Wang and Z. Que, Characteristics and influencing factors of CO_2 emission from inland waters in China, *Sci. China: Earth Sci.*, 2024, **67**(6), 2034–2055.

6 W. Wu, X. Niu, Z. Yan, S. Li, S. A. Comer-Warner, H. Tian, S. L. Li, J. Zou, G. Yu and C. Q. Liu, Agricultural canals are hotspots of greenhouse gas emissions controlled by nutrient input, *Water Res.*, 2023, **242**, 120271.

7 Q. T. Xiao, Z. H. Hu, C. Hu, A. R. M. T. Islam, H. Bian, S. T. Chen, C. Liu and X. H. Lee, A highly agricultural river network in Jurong Reservoir watershed as significant CO_2 and CH_4 sources, *Sci. Total Environ.*, 2021, **769**, 144558.

8 A. V. Borges, F. Darchambeau, T. Lambert, S. Bouillon, C. Morana, S. Brouyere, V. Hakoun, A. Jurado, H. C. Tseng, J. P. Descy and F. A. Roland, Effects of agricultural land use on fluvial carbon dioxide, methane and nitrous oxide concentrations in a large European river, the Meuse (Belgium), *Sci. Total Environ.*, 2018, **610**, 342–355.

9 J. Guo, C. Li, X. B. Xu, M. Sun and L. Zhang, Farmland scale and chemical fertilizer use in rural China: new evidence from the perspective of nutrient elements, *J. Cleaner Prod.*, 2022, **376**, 134278.

10 M. Peacock, J. Audet, D. Bastviken, M. N. Futter and C. D. Evans, Global importance of methane emissions from drainage ditches and canals, *Environ. Res. Lett.*, 2021, **16**(4), 044010.

11 O. Deng, X. Li, L. Deng, S. Zhang, X. Gao, T. Lan, W. Zhou, D. Tian, Y. Xiao, J. Yang, D. Ou and L. Luo, Emission of CO_2 and CH_4 from a multi-ditches system in rice cultivation region: Flux, temporal-spatial variation and effect factors, *J. Environ. Manage.*, 2020, **270**, 110918.

12 Y. Zhang, H. Zhu, B. Yan, X. Li and Y. Ou, Effects of plant and water level on nitrogen variation in overlying and pore water of agricultural drainage ditches in sanjiang plain, northeast China, *Clean*, 2014, **42**(4), 38–392.

13 M. Peacock, J. Audet, D. Bastviken, S. Cook, C. D. Evans, A. Grinham, M. A. Holgerson, L. Hogbom, A. E. Pickard, P. Zielinski and M. N. Futter, Small artificial waterbodies are widespread and persistent emitters of methane and carbon dioxide, *Global Change Biol.*, 2021, **27**(20), 5109–5123.

14 T. Silverthorn, C. Evans and M. Peacock, *Greenhouse gas emissions from drainage ditches and irrigation canals*, Gen. Assembly, 2024, EGU24-8036.

15 S. Teresa, E. Chris and P. Michael, *Greenhouse gas emissions from drainage ditches and irrigation canals*, General Assembly, 2024, vol. **24**, p. , p. 8036.

16 J. H. Zhang, Optimization of Monitoring Points and Model Simulation for Non-point Source Pollution in the Hetao Irrigation District, Master's thesis, Inner Mongolia University, 2022.

17 C. Verpoorter, T. Kutser, D. A. Seekell and L. J. Tranvik, A global inventory of lakes based on high-resolution satellite imagery, *Geophys. Res. Lett.*, 2014, **41**(18), 6396–6402.

18 Y. Gao, S. Y. Wang, Y. Lu, J. B. Liu, L. Y. U. Sidan, K. Sun, J. J. Jia, Z. X. Li and G. R. Yu, Carbon budget and balance critical processes of the regional land water-air interface: Indicating the earth system's carbon neutrality, *Sci. China: Earth Sci.*, 2022, **65**(5), 773–782.

19 A. V. Borges, F. Darchambeau, C. R. Teodoru, T. R. Marwick, F. Tamooh, N. Geeraert, F. O. Omengo, F. Guerin, T. Lambert, C. Morana, E. Okuku and S. Bouillon, Globally significant greenhouse-gas emissions from African inland waters, *Nat. Geosci.*, 2015, **8**(8), 637–642.

20 M. A. Holgerson and P. A. Raymond, Large contribution to inland water CO_2 and CH_4 emissions from very small ponds, *Nat. Geosci.*, 2016, **9**(3), 222–226.

21 Y. Han, Y. Zhai, M. Guo, X. Cao, H. Lu, J. Li, S. Wang and W. Yue, Hydrochemical and Isotopic Characterization of the Impact of Water Diversion on Water in Drainage Channels, Groundwater, and Lake Ulansuhai in China, *Water*, 2021, **13**(21), 30–33.

22 J. R. Li, Study on the Characteristics and Ecological Simulation of Phytoplankton Communities in Ulansuhai Lake, Doctoral Degree, Inner Mongolia Agricultural University, Inner Mongolia, 2014.

23 W. J. Cai and Y. Wang, The chemistry, fluxes, and sources of carbon dioxide in the estuarine waters of the Satilla and Altamaha Rivers, Georgia, *Limnol. Oceanogr.*, 1998, **43**(4), 657–668.

24 Q. T. Xiao, X. F. Xu, H. T. Duan, T. C. Qi, B. Q. Qin, X. Lee, Z. H. Hu, W. Wang, W. Xiao and M. Zhang, Eutrophic Lake

Taihu as a significant CO_2 source during 2000-2015, *Water Res.*, 2020, **170**, 115331.
25 Z. Xu and Y. J. Xu, Dissolved carbon transport in a river-lake continuum: A case study in a subtropical watershed, USA, *Sci. Total Environ.*, 2018, **643**, 640–650.
26 Y. Liao, Q. Xiao, Y. Li, C. Yang, J. Li and H. Duan, Salinity is an important factor in carbon emissions from an inland lake in arid region, *Sci. Total Environ.*, 2024, **906**, 167721.
27 S. Li, R. T. Bush, N. J. Ward, L. A. Sullivan and F. Dong, Air-water CO_2 outgassing in the Lower Lakes (Alexandrina and Albert, Australia) following a millennium drought, *Sci. Total Environ.*, 2016, **542**, 453–468.
28 L. Ran, D. E. Butman, T. J. Battin, X. Yang, M. Tian, *et al.*, Substantial decrease in CO_2 emissions from Chinese inland waters due to global change, *Nat. Commun.*, 2021, **12**(1), 1730.
29 W. S. Zhang and C. J. Song, Spatial distribution and dynamics of lakes in China:Progress in remote sensing monitoring at national scale and new inventory of the maximum lake extent and change trajectory, *Natl. Remote Sens. Bull.*, 2022, **26**(1), 92–103.
30 Y. Gao and G. R. Yu, Regional coupled C-N-H_2O cycle processes and associated driving mechanisms, *Sci. China: Earth Sci.*, 2020, **63**(9), 1227–1236.
31 H. Biswas, S. K. Mukhopadhyay, T. K. De, S. Sen and T. K. Jana, Biogenic controls on the air-water carbon dioxide exchange in the Sundarban mangrove environment, northeast coast of Bay of Bengal, India, *Limnol. Oceanogr.*, 2004, **49**(1), 95–101.
32 P. A. Raymond, J. Hartmann, R. Lauerwald, S. Sobek, C. McDonald, M. Hoover, D. Butman, R. Striegl, E. Mayorga, C. Humborg, P. Kortelainen, H. Duerr, M. Meybeck, P. Ciais and P. Guth, Global carbon dioxide emissions from inland waters, *Nature*, 2014, **507**(7492), 355.
33 W. Y. Duan, Estimation of CO_2 Emission Flux from Lakes on the Qinghai-Tibet Plateau in 2010 and 2020 and Analysis of Its Influencing Factors, Master's thesis, Northwest University, 2022.
34 Y. Wang, W. Z. Yang, Y. Jiao, X. Ma and W. Qi, Quantitative analysis of dissolved carbon sources in the farmland artificial ditch drainage-Lake UlanSuhai continuum in the Hetao Irrigation District's, Inner Mongolia, *J. Hydrol.: Reg. Stud.*, 2024, **55**, 101910.
35 S. Wang, Y. Gao, J. Jia, Y. Lu, J. Wang, X. Ha, Z. Li and K. Sun, Determining whether hydrological processes drive carbon source and sink conversion shifts in a large floodplain-lake system in China, *Water Res.*, 2022, **224**, 119105.
36 P. Kiuru, A. Ojala, I. Mammarella, J. Heiskanen, M. Kamarainen, T. Vesala and T. Huttula, Effects of climate change on CO_2 concentration and efflux in a humic boreal lake: a modeling study, *J. Geophys. Res.: Biogeosci.*, 2018, **123**(7), 2212–2233.
37 G. A. Weyhenmeyer, S. Kosten, M. B. Wallin, L. J. Tranvik, E. Jeppesen and F. Roland, Significant fraction of CO_2 emissions from boreal lakes derived from hydrologic inorganic carbon inputs, *Nat. Geosci.*, 2015, **8**(12), 933–936.
38 G. M. Wilkinson, C. D. Buelo, J. J. Cole and M. L. Pace, Exogenously produced CO_2 doubles the CO_2 efflux from three north temperate lakes, *Geophys. Res. Lett.*, 2016, **43**(5), 1996–2003.
39 D. K. Lv, J. B. Jia, H. X. Yu and Y. Q. Wang, Temporal and spatial variations of CO_2 flux across water-air interface in Nihe reservoir in the boreal zone of China, *Energy Educ. Sci. Technol. A, Energy Sci. Res.*, 2012, **30**(2), 437–444.
40 K. Minkkinen and J. Laine, Vegetation heterogeneity and ditches create spatial variability in methane emissions from peatlands drained for forestry, *Plant Soil*, 2006, **285**(1–2), 289–304.
41 A. P. Schrier-Uijl, P. S. Kroon, P. A. Leffelaar, J. C. van Huissteden, F. Berendse and E. M. Veenendaal, Methane emissions in two drained peat agro-ecosystems with high and low agricultural intensity, *Plant Soil*, 2010, **329**(1–2), 509–520.
42 L. L. Tian, H. Akiyama, B. Zhu and X. Shen, Indirect N_2O emissions with seasonal variations from an agricultural drainage ditch mainly receiving interflow water, *Environ. Pollut.*, 2018, **242**, 480–491.
43 Q. Yang, S. Chen, Y. Li, B. Liu and L. Ran, Carbon Emissions from Chinese Inland Waters: Current Progress and Future Challenges, *J. Geophys. Res.: Biogeosci.*, 2024, **129**(2), e2023JG007675.
44 J. H. Park, O. K. Nayna, M. S. Begum, E. Chea and J. Hartmann, Reviews and syntheses: Anthropogenic perturbations to carbon fluxes in Asian river systems - concepts, emerging trends, and research challenges, *Biogeosciences*, 2018, **15**(9), 3049–3069.
45 E. H. Stanley, N. J. Casson, S. T. Christel, J. T. Crawford, L. C. Loken and S. K. Oliver, The ecology of methane in streams and rivers: patterns, controls, and global significance, *Ecol. Monogr.*, 2016, **86**(2), 146–171.
46 Q. T. Xiao, X. F. Xu, T. C. Qi, J. H. Luo, X. H. Lee and H. T. Duan, Lakes shifted from a carbon dioxide source to a sink over past two decades in China, *Sci. Bull.*, 2024, **69**(12), 5.
47 S. Larsen, T. Andersen and D. O. Hessen, The pCO_2 in boreal lakes: organic carbon as a universal predictor?, *Global Biogeochem. Cycles*, 2011, **25**(2), GB2012.
48 M. Rodriguez, T. Gonsiorczyk and P. Casper, Methane production increases with warming and carbon additions to incubated sediments from a semiarid reservoir, *Inland Waters*, 2018, **8**, 109–121.
49 P. S. Keller, N. Catalan, D. von Schiller, H. P. Grossart and M. Koschorreck, Global CO2 emissions from dry inland waters share common drivers across ecosystems, *Nat. Commun.*, 2020, **11**(1), 2126.
50 P. Bodmer, M. Heinz, M. Pusch, G. Singer and K. Premke, Carbon dynamics and their link to dissolved organic matter quality across contrasting stream ecosystems, *Sci. Total Environ.*, 2016, **553**, 574–586.
51 G. Abril, S. Bouillon, F. Darchambeau, C. R. Teodoru, T. R. Marwick and F. Tamooh, Technical note: large overestimation of pCO_2 calculated from ph and alkalinity

in acidic, organic-rich freshwaters, *Biogeosciences*, 2015, **12**(1), 67–78.

52 M. B. Wallin, S. Löfgren, M. Erlandsson and K. Bishop, Representative regional sampling of carbon dioxide and methane concentrations in hemiboreal headwater streams reveal underestimates in less systematic approaches, *Global Biogeochem. Cycles*, 2014, **28**(4), 465–479.

53 T. K. Kratz, J. Schindler, D. Hope, J. L. Riera and C. J. Bowser, Average annual carbon dioxide concentrations in eight neighboring lakes in northern Wisconsin, USA, *Verh. Int. Ver. Theor. Angew. Limnol.*, 1995, **26**(2), 335–338.

54 P. A. Raymond, N. F. Caraco and J. J. Cole, Carbon dioxide concentration and atmospheric flux in the Hudson River, *Estuaries*, 1997, **20**(2), 381–390.

55 R. Wanninkhof, Relationship between wind speed and gas exchange over the ocean revisited, *Limnol. Oceanogr.: Methods*, 2014, **12**(6), 351–362.

56 S. R. Alin, M. F. F. L. Rasera, C. I. Salimon, J. E. Richey, G. W. Holtgrieve, A. V. Krusche and A. Snidvongs, Physical controls on carbon dioxide transfer velocity and flux in low-gradient river systems and implications for regional carbon budgets, *J. Geophys. Res.: Biogeosci.*, 2011, **116**, G01009.

57 J. Y. Zhu, K. Peng, Y. Y. Li, C. R. Liu and L. Zhou, Characteristics and Influencing Factors of Carbon Dioxide Emission Flux in Hongze Lake under Different Hydrological Scenarios, *J. Lake Sci.*, 2022, (004), 034.

58 T. C. Qi, Q. T. Xiao, Y. Q. Miao and H. T. Duan, Spatio-Temporal Distribution Characteristics of Carbon Dioxide Concentration and Its Water-Air Exchange Flux in Chaohu Lake, *J. Lake Sci.*, 2019, **31**(03), 766–778.

59 Y. G. Chen, X. H. Li, Z. X. Hu, W. L. Liu and W. P. Hu, CO_2 Flux Across the Water-Air Interface in Eight Major Lakes in China During Winter, *Appl. Ecol. Environ. Sci.*, 2006, **15**(4), 665–669.

60 X. Q. Liu, Study on characteristics of greenhouse gas emissions and driving mechanisms in Baiyangdian Wetland, Master's thesis, Hebei University, 2024.

61 L. Wang, C. D. Xiao, Z. H. Du, D. T. Maher, J. F. Liu and Z. Q. Wei, In situ measurement on air water flux of CH_4, CO_2 and their carbon stable isotope in lakes of northeast Tibetan Plateau, *Adv. Clim. Change Res.*, 2022, **13**(2), 279–289.

62 S. Li, R. T. Bush, I. R. Santos, Q. Zhang, K. Song, R. Mao, Z. Wen and X. X. Lu, Large greenhouse gases emissions from China's lakes and reservoirs, *Water Res.*, 2018, **147**, 13–24.

63 D. Bastviken, L. J. Tranvik, J. A. Downing, P. M. Crill and A. Enrich-Prast, Freshwater Methane Emissions Offset the Continental Carbon Sink, *Science*, 2011, **331**(6013), 50.

64 N. Barros, J. J. Cole, L. J. Tranvik, Y. T. Prairie, D. Bastviken, V. L. M. Huszar, P. del Giorgio and F. Roland, Carbon emission from hydroelectric reservoirs linked to reservoir age and latitude, *Nat. Geosci.*, 2011, **4**(9), 593–596.

65 L. Ran, X. X. Lu, H. Yang, L. Li, R. Yu, H. Sun and J. Han, CO_2 outgassing from the Yellow River network and its implications for riverine carbon cycle, *J. Geophys. Res.: Biogeosci.*, 2015, **120**(7), 1334–1347.

66 F. Wang, Y. Wang, J. Zhang, H. Xu and X. Wei, Human impact on the historical change of CO_2 degassing flux in River Changjiang, *Geochem. Trans.*, 2007, **8**(1), 7.